Neurochemical Research (2019) 44:1410–1424
https://doi.org/10.1007/s11064-019-02721-8

ORIGINAL PAPER

Inflammation in Traumatic Brain Injury: Roles for Toxic A1 Astrocytes and Microglial–Astrocytic Crosstalk

David P. Q. Clark[1] · Victoria M. Perreau[1] · Sandy R. Shultz[2,3] · Rhys D. Brady[2,3] · Enie Lei[1] · Shilpi Dixit[1] · Juliet M. Taylor[4] · Philip M. Beart[1,4] · Wah Chin Boon[1]

Received: 28 July 2018 / Revised: 7 January 2019 / Accepted: 8 January 2019 / Published online: 19 January 2019

Abstract

Traumatic brain injury triggers neuroinflammation that may contribute to progressive neurodegeneration. We investigated patterns of recruitment of astrocytes and microglia to inflammation after brain trauma by firstly characterising expression profiles over time of marker genes following TBI, and secondly by monitoring glial morphologies reflecting inflammatory responses in a rat model of traumatic brain injury (i.e. the lateral fluid percussion injury). Gene expression profiles revealed early elevation of expression of astrocytic marker glial fibrillary acidic protein relative to microglial marker allograft inflammatory factor 1 (also known as ionized calcium-binding adapter molecule 1). Adult rat brains collected at day 7 after injury were processed for immunohistochemistry with allograft inflammatory factor 1, glial fibrillary acidic protein and complement C3 (marker of bad/disruptive astrocytic A1 phenotype). Astrocytes positive for glial fibrillary acidic protein and complement C3 were significant increased in the injured cortex and displayed more complex patterns of arbourisation with significantly increased bifurcations. Our observations suggested that traumatic brain injury changed the phenotype of microglia from a ramified appearance with long, thin, highly branched processes to a swollen amoeboid shape in the injured cortex. These findings suggest differential glial activation with astrocytes likely undergoing strategic changes in morphology and function. Whilst a detailed analysis is needed of temporal patterns of glial activation, ours is the first evidence of a role for the bad/disruptive astrocytic A1 phenotype in an open head model of traumatic brain injury.

Keywords Traumatic brain injury · Inflammation · Astrocyte · Toxic phenotype · Glial crosstalk

Abbreviations

A1	Neurotoxic phenotype of reactive astrocytes
A2	Neuroprotective phenotype of reactive astrocytes
Aif1	Allograft inflammatory factor 1
AuD	Auditory cortex
BBB	Blood–brain barrier
BDNF	Brain-derived neurotrophic factor
C3	Complement component 3
C3+	Complement component 3 immunoreactive positive
CCI	Controlled cortical impact injury
CNS	Central nervous system
CSPG	Chondroitin sulphate proteoglycan
C1q	Complement component 1q
CD68	Cluster of differentiation 68
CSF-1	Colony stimulating factor 1
DAMPs	Damage-associated molecular patterns
DAM	Disease-associated microglia
DAPI	4′-6-diamidino-2-phenylindole
FPI	Lateral fluid percussion injury
GFAP	Glial fibrillary acidic protein
GFAP+	Glial fibrillary acidic protein immunoreactive positive
HCl	Hydrochloric acid

David P. Q. Clark and Victoria M. Perreau have contributed equally to this manuscript.

Special issue in honor of Prof. Anthony J. Turner.

✉ Philip M. Beart
philip.beart@florey.edu.au

[1] The Florey Institute of Neuroscience and Mental Health, Parkville, VIC 3051, Australia

[2] Department of Neuroscience, Central Clinical School, Monash University, Melbourne, VIC 3004, Australia

[3] Department of Medicine, The Royal Melbourne Hospital, The University of Melbourne, Parkville, VIC 3052, Australia

[4] Department of Pharmacology & Therapeutics, University of Melbourne, Parkville, VIC 3010, Australia

Iba1	Ionized calcium-binding adapter molecule 1
IL	Interleukin
M1	Neurotoxic phenotype of reactive microglia
M2	Neuroprotective phenotype of reactive microglia
NDS	Normal donkey serum
PBS	Phosphate buffered saline
S2	Region somatosensory cortex
Sham	Sham-injury
TBI	Traumatic brain injury
TGF-β	Transforming growth factor beta 1
TNF	Tumor necrosis factor

Introduction

Traumatic brain injury (TBI) is a leading cause of accident-related hospital admissions and internationally a leading cause of disability and death in children and young adults, and is now recognized as a major public health problem. Indeed, the loss of productive life and the economic costs to society in general as a consequence of TBI are massive. The World Health Organization emphasizes that the world faces an epidemic of road traffic accidents in developing countries by 2020, and that like all neurological disorders progress is desperately needed in prevention and intervention (http://www.who.int/mental_health/publications/neurological_disorders_ph_challenges/en/). Moreover, it is only recently that repeated mild TBI, like a single episode of severe TBI, has been recognized to result in debilitating neurodegenerative processes [1]. Clearly the path to improved interventions and the reduction of the subsequent severity of TBI-induced injury requires basic and clinical insights, and only with an improved understanding of the pathological mechanisms can effective drug discovery progress successfully. Whilst TBI is extremely heterogeneous (in terms of its nature and extent) and can cover a continuum of injury from "focal" to "diffuse", it is generally accepted that there is temporal progression of pathology involving degeneration and inflammation [2]. In the more recent literature, there has been a growth of interest in the role of inflammation beyond the acute phase, with much attention currently focusing on different inflammatory responses in long-term chronic outcomes post-TBI [3].

In TBI, neuroinflammation can potentially play detrimental and/or beneficial roles [4], as dictated by the progress of injury [5, 6]. Neuroinflammation following brain injury is a necessary process to remove necrotic debris and repair tissue, but may exacerbate the injury if dysregulated [7]. A trauma to the brain induces an immediate disruption of the blood-brain barrier (BBB) and allows the infiltration of the circulating macrophages and neutrophils to clear necrotic debris (phagocytosis). In the process, these immunocytes release pro-inflammatory molecules such as interleukins (ILs), tumor necrosis factor (TNF), etc. [8]. The increase in pro-inflammatory molecules recruits additional immunocytes to the site and exacerbates the secondary insult response [9]. In addition to the infiltration of immune cells, the activation of the local microglia and astrocytes plays a major role in the response to brain injury [10]. Microglia and astrocytes are abundant specialised central nervous system (CNS) cells that provide trophic support to neurons, regulating the function and formation of synapses and contributing to homeostatic regulation [11]. However, there is a growing body of evidence which indicates that activated microglia and astrocytes have a potential loss of supporting function and a gain of abnormal effects that lead to pathological changes in CNS tissue after brain injury [12, 13]. Persistent inflammation has indeed been linked to both post-traumatic neurodegeneration and functional deficits in a number of preclinical [14–17] and clinical studies [3, 9].

Following TBI, healthy astrocytes transform into 'reactive astrocytes' characterised by molecular and functional changes together with variability in cellular hypertrophy. These reactive astrocytes enmesh the lesion site and deposit an inhibitory extracellular matrix consisting primarily of chondroitin sulphate proteoglycan (CSPG) that contributes to the formation of glial scarring [18]. In cases of mild to moderate insult, reactive astrocytosis is triggered but there is a potential for resolution if the insult is removed. By contrast, in severe brain injury reactive astrocytes quickly enmesh the site of the injury, forming a barrier known as the glial scar to protect healthy tissue from nearby areas of intense neuroinflammation. It was thought that this mechanism of the CNS to isolate the damaged region from the normal functioning neurons created an impermissible environment for neural repair or axonal regeneration [19]. However, recent evidence showed that the inhibition of glial scarring neither resulted in axonal regeneration nor reduction in CSPG [20]. Anderson et al. proposed that astrocyte scar formation may aid rather than prevent CNS axon regeneration [20].

Recent compelling evidence from studies investigating neurodegenerative diseases indicates that neuroinflammation and ischemic conditions in the CNS induce two distinct phenotypes of reactive astrocytes, termed A1 and A2 phenotypes. The A1 phenotype being harmful, and contributing to neuronal death, whereas the A2 phenotype may be neuroprotective [21]. Complement component 3 (C3) is one of the most characteristic and highly upregulated genes in A1 astrocytes and is not expressed by the A2 reactive astrocytes [21]. The complement system is a protein cascade involved in the innate immune response that has been implicated in exacerbating neuroinflammation in Alzheimer's disease, Huntington's disease, Parkinson's disease, amyotrophic lateral sclerosis, and multiple sclerosis [22]. However, the A1

and A2 phenotypes of reactive astrocytes (such as the immunostaining for C3) following TBI have yet to be reported.

Like astrocytes, microglia display great heterogeneity in inflammatory responses. The duality of microglial responses is well established and led to the definition of M1 and M2 phenotypes [4, 23], although the current view of microglial responses and phenotypes has shifted to favour a continuum of responses wherein M1 and M2 states represent the two extreme phenotypes, "bad/pro-damage" and "good/pro-repair" [24]. Microglial cells, which normally help attenuate neuroinflammation [7] can become over-activated and release pro-inflammatory compounds (e.g. ILs, TNF), nitric oxide and reactive oxygen species which are cytotoxic to cells [4, 24–26]. In a recent study, microglia were shown to be capable of inducing the A1 reactive phenotype of astrocytes via the release of pro-inflammatory compounds, which further contribute to the cytotoxic environment [21].

So the recent emergence of the A1/A2 concept for astrocytic phenotypes [21] is hardly surprising given the earlier evidence from genomic analyses published from the same laboratory [27] and the considerable existent literature on astrocytes possessing diverse morphologies and biologies. There remain numerous unknowns here, and it is very likely that astrocytic responses also exist across a diverse continuum [28].

We hypothesised that A1 and A2 astrocytic phenotypes characterised in neurodegenerative disease would also play an important role in response to TBI. We have used a combination of targeted reanalysis of publically available TBI gene expression data to investigate the astrocytic and microglial gene profiles and original experiments to investigate the morphology of astrocytes and microglia in TBI. Our experimental analyses included immunohistochemistry and stereology in a rat lateral fluid percussion injury model (FPI). We used glial fibrillary acidic protein (GFAP) and allograft inflammatory factor 1 (Aif1), also known as ionized calcium-binding adapter molecule 1 (Iba1), as markers for astrocytes and microglia respectively. Our analysis (1) identified patterns of differential activation of astrocytes and microglia in TBI; (2) how these insights have driven our initial studies of inflammation and A1 astrocytes in a rodent model of TBI, and (3) placed our observations in the context of the emergent literature on the roles of neuroinflammation in TBI.

Materials and Methods

Materials

Antibodies rat anti-GFAP (13-0300) and Alexa Fluor 488 conjugated donkey anti-rabbit (A21206) were purchased from Thermofisher; rabbit anti-Iba1 (019-19741) from Wako; rabbit anti-C3 (BS8557) from Bioworld Tech; Alexa Fluor 594 conjugated goat anti-rat (ab15160) from Abcam. Normal donkey serum (NDS) was purchased from Chemicon; DAPI (4′-6-diamidino-2-phenylindole) from Vector Laboratories; DAKO fluorescent mounting medium from Agilent. Other non-specified reagents are purchased from Sigma-Aldrich.

Reanalysis of Public Gene Expression Data Following TBI

Published microarray data examining gene expression in both mouse and rat models of head trauma (lateral fluid percussion-induced brain injury in rats and lateral controlled cortical impact injury (CCI) in mice) [29] were downloaded from Gene Expression Omnibus [30] GSE2392. The publically available data include a single control group, and sham and injury groups across multiple time points with 2–5 biological replicates for each treatment group. For the rat data; control n = 3, sham n = 4 for 0.5 h, and 4 h and n = 2 for 8 h, 24 h and 72 h, injury groups are n = 5 for 0.5 h, n = 3 for 4 h, 8 h, 24 h and 72 h. For the mouse data; control and sham groups are n = 2 for all time points and for injury groups n = 3 for all time points.

Cel files were analysed using the RMA algorithm and background corrected [31] in Partek Genomics Suite (6.16.0419). Probesets were annotated with the RG_U34A.na36.annot.csv and MG_U74Av2.na36.annot.csv annotation files for the Rat and Mouse data respectively. An ANOVA on time and treatment was performed and the log base 2 LS mean expression values and standard errors for selected probe sets of interest were plotted in RStudio (1.0.153) [32] using R (3.4.0), and ggplot2 (2.2.1) [33].

Where multiple probe sets were available for a gene of interest comparable mouse and rat probe sets were selected if they targeted the same region in the gene of interest. Target regions of probe sets were retrieved from the Netaffx analysis site (Affymetrix.com) and aligned to the mouse mm9 or rat rn4 genome using the Blat tool in UCSC genome browser [34, 35]. In this way comparable probe sets from two different array platforms and species were identified and are detailed in Table 1.

Animals

Adult male Sprague Dawley rats were purchased from the Monash Animal Research Services (Melbourne, Australia). Rats were 11 week-old and weighing 260–360 g by the time of the study. Animals were group-housed under a 12 h light/dark cycle before the surgery and individually housed after the surgery. Animals had free access to food and water ad libitum for the duration of the study. Animal handling techniques were conducted in compliance with the National

Table 1 Probe sets and gene target regions

Species/array	Gene	Probe set	Gene target region
Rat/RG-U34A	*Gfap*	AF028784cds#1_s_at	Coding region and 3′UTR of transcript variant 2
Mouse/MU74A_v2	*Gfap*	94143_at	3′UTR of transcript variant 2
Rat/RG-U34A	*Aif1* (*Iba1*)	U17919_s_at	All coding exons and some 5′ and 3′ UTR
Mouse/MU74A_v2	*Aif1* (*Iba1*)	102330_at	Some 5′UTR and the first 5 coding exons
Rat/RG-U34A	*C3*	X52477_at	Last two coding exons
Mouse/MU74A_v2	*C3*	93497_at	Last three coding exons
Rat/RG-U34A	*Bdnf*	RC_AI030286_S_AT	Near 3′UTR
Mouse/MU74A_v2	*Bdnf*	102727_at	Near 3′UTR

Health and Medical Research Council (Australia) guidelines for the Care and Use of Laboratory Animals and experimental procedures were approved by the Florey Animal Ethics Committee. Rats were randomly assigned to receive either a sham-injury (n = 5) or a lateral fluid percussion injury (n = 5).

Surgical Procedures

FPI and sham procedures were performed based on a previously described standard protocol [36]. Briefly, in a tightly sealed box, anaesthesia was induced with 4% isoflurane and 2 L/min oxygen flow. Under aseptic conditions, a craniotomy (3 mm diameter window; 3.0 mm posterior and 4.0 mm lateral to the left of bregma) was performed to expose the intact dura mater of the brain. A hollow plastic injury cap was then sealed over the craniotomy with dental cement and cyanoacrylate, and secured to the skull with three small stainless steel screws. At first response of a hind-limb withdrawal, a single FPI was given to the experimental TBI group with a force of 2.5–3.0 atm (moderate injury). This percussion force has been shown to elicit a robust neuroinflammatory response and behavioural deficits [14, 37, 38]. The injury cap was removed and incisions were sutured upon spontaneous breathing. Sham-injury rats underwent the same procedures with the exception that they did not receive the fluid pulse.

To assess the acute severity of the injury, apnoea, unconsciousness and self-righting reflex times were monitored immediately post-surgery [14, 37]. Apnoea is the time taken for the animal to regain spontaneous breathing. Unconsciousness was the period from the injury to a hind-limb withdrawal response to a toe pinch. Self-righting is the time that the animal takes to return to an upright position from the injury.

Brain Collection and Sectioning

On day 7 after the surgery, rats were killed with a lethal dose of sodium pentobarbitone (150 mg/kg) via intraperitoneal injection and brains were immediately collected. Brains were washed with 0.9% NaCl to remove blood and debris before they were snap-frozen on dry ice while fully submerged in 2-methylbutane for approximately 15 s. Brains were then stored at − 20 °C before sectioning. Using the cryostat (Leica RM2165, Nussloch, Germany), coronal brain sections (20 µm thick) were collected in series of four so that consecutive sections were 80 µm apart. A total of six sections were slide-mounted onto a single Superfrost Plus + coated slide (Menzel-Glazerâ, Germany) with a frozen sliding microtome. Slide-mounted sections then fixed in cold acetone for 5 min once they were dry after cutting and stored at − 20 °C until further analysis.

Immunohistochemistry

Sections between bregma − 2.56 and − 3.94 mm [39] were used to perform immunohistochemistry, and a total of n = 5 rats from each of the treatment groups were examined. All sample sections were stained and imaged at the same time. Double labelling was used to determine whether brain injury influenced the total expression of astrocytic cells and reactive astrocytes, brain sections were double-stained with rat anti-GFAP and rabbit anti-C3, marker for reactive A1 phenotype of astrocytes [21], or rabbit-anti Aif1/Iba1 (marker for microglia [40]) primary antibodies.

Sections were washed with 1 × Phosphate Buffered Saline (PBS) to rehydrate (× 3, 5 min). Sections were then fixed in 2% paraformaldehyde and retrieved epitopes with 2 M hydrochloric acid (HCl) for 30 min at 40 °C and 0.1 M borate buffer (pH 8.5) for 20 min at room temperature to neutralise HCl. Non-specific binding and membrane permeabilization was performed with 5% NDS, 0.1% Triton X-100 in PBS for 15 min. Sections were then incubated in rat anti-GFAP and rabbit anti-C3, or rabbit anti-Iba1/Aif1 (1:1000; Wako) primary antibodies overnight at 4 °C, followed by incubating with Alexa Fluor 594 conjugated goat anti-rat (1:250; ab15160, Abcam) and Alexa Fluor 488 conjugated donkey anti-rabbit (1:250; A21206, Thermofisher) secondary antibodies for 1 h at room temperature. Sections then counterstained with DAPI (Vector Laboratories) and coverslipped with DAKO (Agilent) mounting medium. Specific

immunoreactivity was also tested as mentioned above. Primary and secondary antibodies were diluted in 5% NDS, 0.1% Triton X-100 in PBS. After each step, sections were washed with 1 × PBS. Stained tissue sections were analysed using stereology as described in the following sections.

Stereology

Unbiased estimation of the number of GFAP+ cells and C3+ cells in the cortex of the injured hemisphere (ipsilateral side) was obtained with stereological analysis using the light/fluorescent microscope Olympus BX-51 (Olympus Corp.) with a Qimaging camera system, the images were first captured using automated settings to optimise resolution and then used the same setting for all subsequent slides.. All stereological analyses were performed using a computer-assisted stereological system with a motorized stage and the commercially available StereoInvestigator software (MicroBrightField Bioscience, Williston, VT). Due to the variability of the border between the somatosensory cortex (S2 region) and the auditory cortex (AuD) between bregma −2.56 and −4.14 mm (according to the Paxinos and Watson rat brain atlas) [39], the contour of the counting region in the cortex was defined by the midline of the brain section to approximately lateral to the tip of the hippocampus. Section boundaries were mapped using a Plan ×2 (NA = 0.05) magnification air lens and the number of cells were counted using a UPlan Apo ×40 air lens (NA = 0.75). A pilot study was performed to determine the size of the counting frame (150 µm × 150 µm), grid spacing at intervals along the x and y axes (870 µm × 870 µm), probe height (12 µm) with dual guard zone height (4 µm), while maintaining an acceptably low coefficient of error [Gundersen (m = 1); 1st Schmitz and Hof; 2nd Schmitz and Hof CE are all < 0.10] [41, 42]. Counting was performed on all 6 sections for each animal, with an average sampling of 3% of the total mapped area per hemisphere.

Estimation of GFAP+ and C3+ cells density

DAPI stained nuclei were used to identify the centre of each GFAP+ and C3+ labelled astrocytes. The astrocyte was only counted if the nucleus associated with that astrocyte first came into focus within the optical dissector counting frame. Any astrocyte with a nucleus that touched the left or bottom side of the dissector frame or came into focus in the guard zones was not counted to avoid errors in population estimation. Population estimation was worked out using the general formula:

$$\text{Total population} = \text{total cells counted} \times 1/ssf \times 1/asf \times 1/hsf,$$

where ssf is the sampling subfraction, asf is the area subfraction and hsf is the height subfraction. The number of GFAP+ and C3+ cells expressed per mm^3 was worked out by dividing the estimated total population of each fluorescent labelled cell (GFAP+ or C3+) by the volume of the contour for the counted sections.

Cell Tracings

To compare the morphology of GFAP+/C3− and GFAP+/C3+ astrocytes, cells were randomly chosen in the cortex and at least three sections per animal were used. Cells were observed with the light/fluorescent microscope Olympus BX-51 (Olympus Corp.) using a ×63 oil objective.

Real-time images were digitized by a Qimaging digital camera system and cells were traced using Neurolucida software (Microbrightfield, Inc., Williston, USA). For each cell traced, Neurolucida Explorer (Microbrightfield, Inc., Williston, USA) calculated the total process length, the total number of nodes. Arbour branch complexity was calculated using Sholl analysis with concentric circles drawn every 5 µm from the cell body.

Statistical Analysis

For the public gene expression data analysis, each time point was compared between the sham and TBI groups using ANOVA contrast. For the histochemical studies, data were analysed using non-parametric *t* test (Mann–Whitney, Graphpad Prism 7.0 software, San Diego, CA, USA) between injury and sham groups due to small sample size. All data were expressed as mean ± SEM. $p < 0.05$ were considered as significant and indicated by an asterisk (*), $p < 0.01$ and $p < 0.001$ as highly significant and are indicated by ** and *** respectively, whereas $p < 0.0001$ as extremely significant and indicated by **** in the graphs.

Results

Expression Profiles of Marker Genes in Rat and Mouse Models of Head Trauma

Despite differences in head trauma models, species, and microarray platforms the expression profiles over time of target genes of interest are well conserved between species. As previously reported by Natale et al. [29], there is a significant increase in *Gfap* expression (marker of astrocyte reactivity) in both rat FPI (Fig. 1a) and mouse CCI (Fig. 1b) models as early as 8 h when compared to the sham animals. At the same time point, we observed a concomitant increase in C3 expressions in both TBI models (Fig. 1e, f). Although *Gfap* levels increased over time and remain at maximal levels at 72 h, *C3* levels remained fairly constant. Surprisingly, *Aif1/Iba1* expression (marker of microglia reactivity) begins

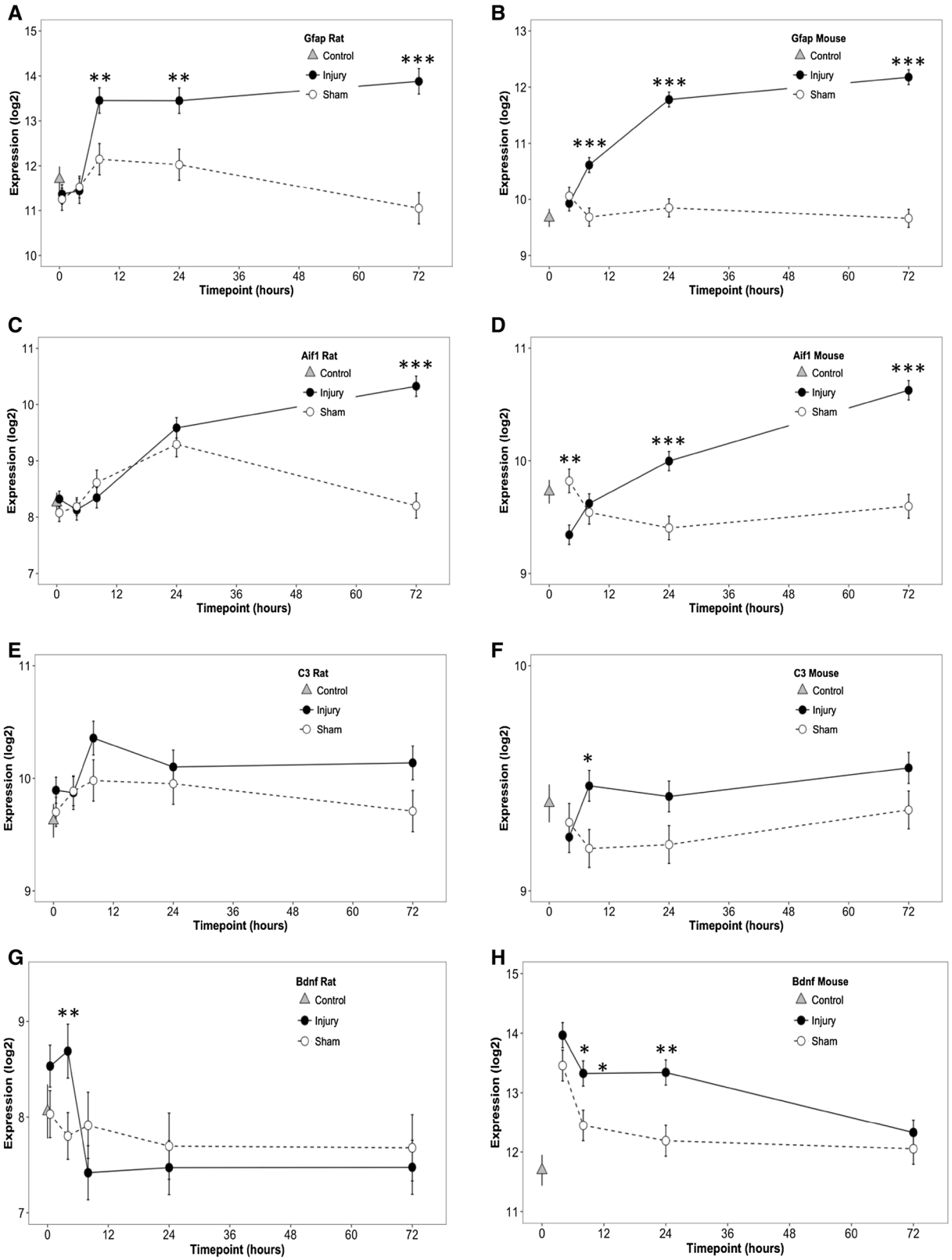

Fig. 1 Gene expression profiles for *Gfap, Aif1, C3* and *Bdnf* in mouse and rat parieto-occipital cortices (containing the contrusion) following head trauma. Gene expression for sham and injured animals was measured at 30 m, 4 h, 8 h, 24 h, and 72 h for rat and 4 h, 8 h, 24 h, and 72 h for mouse data. Expression value shown is Log base2 of Least Squares mean (LS mean) and error bars are standard error of LS mean. Full details are given in the text, and for the probe sets used for each gene and their target regions see Table 1. $*p<0.05$, $**p<0.01$, $***p<0.001$ (ANOVA contrast) between TBI and Sham groups at that time point

to exhibit a difference from the sham animals at a slightly later time point than *Gfap* (significant at 24 h in the mouse CCI model) but like *Gfap* remains maximal at 72 h in both the mouse CCI model and rat FPI model (Fig. 1c, d). Brain-derived neurotrophic factor (*Bdnf*) expression increases very early following injury at 4 h and is already returning to normal levels by 8 h (Fig. 1g, h).

GFAP+ Astrocyte Populations in the Cortex of Sham and TBI Animals

When comparing GFAP+ astrocyte populations in the contralateral and ipsilateral hemispheres according to the type of injury (sham or TBI), the ipsilateral hemisphere showed a relatively larger estimated population of GFAP+ astrocytes ($p < 0.01$, Fig. 2), indicating more neuroinflammation on the injured hemisphere as expected. Surprisingly, a sham injury (on the ipsilateral cortex) was enough to initiate neuroinflammation, shown by an increase in the estimated population of GFAP+ astrocytes when compared to the contralateral cortex ($p < 0.05$, Fig. 2).

When comparing the ipsilateral hemispheres, a statistically significant increase in the population of GFAP+ astrocytes was observed between the TBI animals and the sham-injury animals ($p < 0.01$, Fig. 2). Moreover, C3-labelling of GFAP+ cells, which were presumed to be astrocytes based on their morphology and confirmed in Fig. 3 (*vide infra*), indicated that A1 astrocytes were significantly elevated in ipsilateral versus contralateral cortex ($p < 0.05$, Fig. 2) of the TBI rats. In the sham animals, there was no change in the induction of the A1 astrocyte phenotype on the ipsilateral and the contralateral cortex ($p > 0.05$, Fig. 2). Note that we did not detect any C3+ cells which were not GFAP+ although not all GFAP+ cells are C3+.

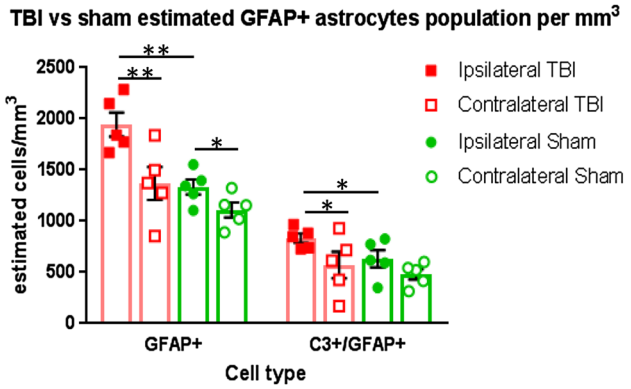

Fig. 2 Effects of traumatic brain injury on the estimated populations of **a** GFAP+ astrocytes and **b** GFAP+ astrocytes with A1 phenotype (C3+). Values are shown as the estimated population of mean ± SEM, Kruskal–Wallis test with post hoc *t* test was performed. n = 5 for each animal group

Morphology of GFAP+/C3+ to GFAP+/C3− labelled astrocytes

In the present study, immunofluorescence staining of C3 is along the processes and somata of hypertrophic GFAP+ astrocytes in rat brains (Fig. 3). When the astrocytes were traced with the Neurolucida software in real-time, across the depth of histological sections we were able to elucidate the complexity of the arbour. When comparing the arbour complexity of GFAP+/C3+ to GFAP+/C3− labelled astrocytes (Fig. 4a, b), GFAP+/C3+ astrocytes (Fig. 4a) showed a more complex pattern of arbourisation characterised by more numerous branches and a higher number of branching points. Tracing of GFAP+/C3+ cells showed a statistically significant increase in the total astrocyte process length relative to GFAP+/C3− astrocytes, ($p < 0.05$) (Fig. 4c). In addition, GFAP+/C3+ traced cells also showed more numerous bifurcation points, shown as the number of nodes (Fig. 4d). This morphological index also showed a statistical significant difference ($p < 0.05$). Sholl analysis of the two subtypes of astrocytes by generation of concentric circles in 5 µm increments from the soma of the cell revealed a significant increase in the number of bifurcations ($p < 0.05$) when comparing GFAP+/C3+ astrocytes to GFAP+/C3− (see Fig. 4e).

Morphology of Aif1/Iba1+ labelled microglia

In our immunohistochemical studies (Fig. 5), we observed that Aif1/Iba1 was expressed in the cytoplasm of the microglia. Aif1/Iba1+ cells in the TBI brains have assumed a swollen amoeboid shape whereas the Aif1/Iba1+ cells in the sham brain have a ramified appearance with long thin processes.

Discussion

Whilst TBI is extremely heterogeneous, what is becoming clear from recent animal studies is that the nature and extent of the inflammatory response involving microglia and astrocytes is quite variable, being dependent upon the model employed and whether the injury employed is acute, subacute or long term and single or repeated insults (reviewed by [5]). Our aim was to assess the involvement of glial populations in TBI. These initial studies reported herein illustrate our multi-faceted approach, which is both theoretical and animal-based in trying to dissect underlying mechanisms contributing to neuroinflammation. To support our findings we executed a targeted reanalysis of publically available genome wide expression data examining TBI. These data show distinct expression profiles over time for the astrocytic marker GFAP and microglial marker Aif1/Iba1, with both

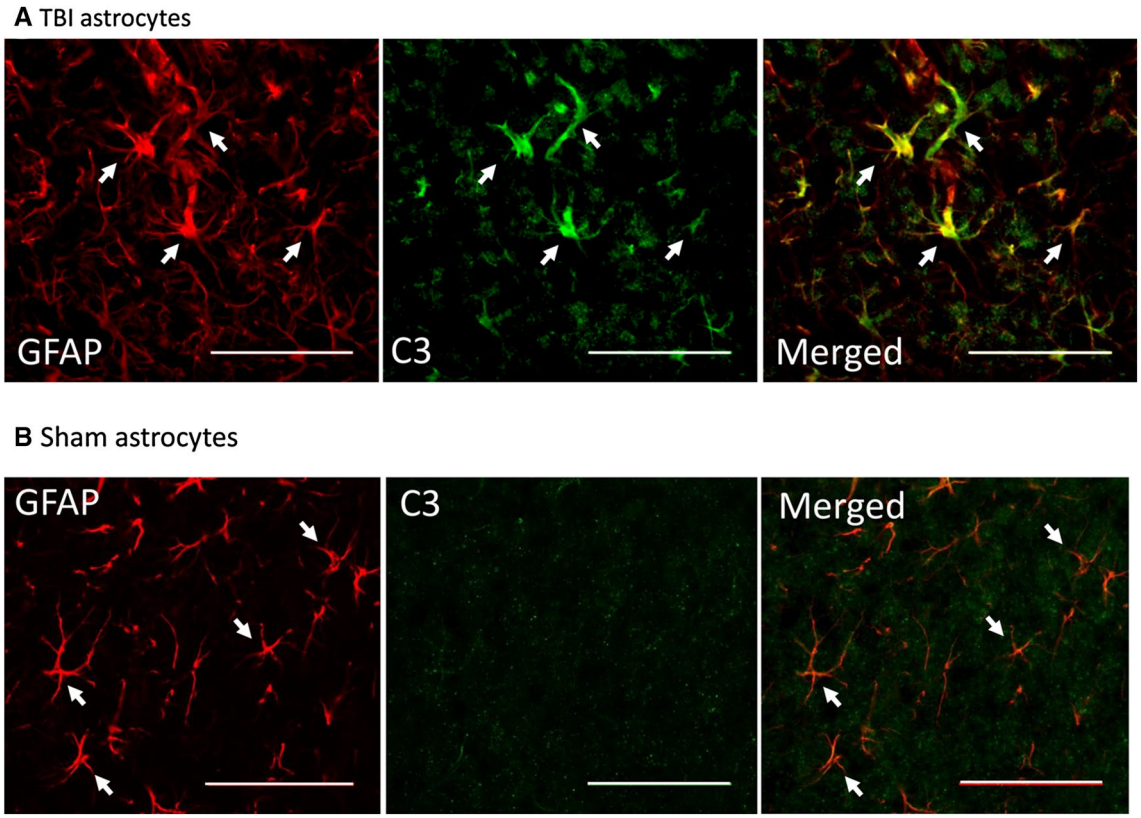

Fig. 3 Immunofluorescent labelling of GFAP and C3 in the cortex of **a** TBI; **b** Sham rats. Immunolabelled for GFAP (red) and C3 (green); merged images showing the co-localisation of GFAP and C3. Arrow heads indicate astrocytes of interest. All scale bars shown are 100 µm. In the sham sample image, no C3+ cells were observed. Images show representative example of results obtained on n = 5 mice

genes exhibiting maximal increase in injury groups compared to sham at the latest time point (72 h). The astrocytic marker GFAP and A1 astrocytic marker C3 were upregulated at 8 h after injury, whereas the microglial marker was upregulated at 24 h after injury—indicating that astrocytes may be activated before the microglia. These expression profiles are largely conserved between different injury models and species (rat FPI vs. mouse controlled cortical impact models). These expression profiles are in contrast to the previous report by Liddelow et al. [21] which proposed that the microglia can activate astrocytes—as demonstrated by the fact that astrocytes were activated by the lipopolysaccharide activated microglia-conditioned medium. Existent literature suggests that there are multiple phases of glial crosstalk in TBI [5], a concept which is discussed in detail below. Nonetheless, we proceeded to explore glial phenotypes in the FPI model and here we found what we believe is the first evidence for toxic, C3-labelled A1 astrocytes in an open head model of TBI. Our analyses of these related events, and especially the time-dependent changes in the different glial populations, are at an early stage and moving forward we plan to fully dissect the related glial mechanisms underpinning inflammation in TBI.

BDNF may also be involved in the "good/beneficial" response of astrocytes as we have previously found its expression is elevated in healthy astrocytes in vitro in a phenotype we termed "pro-survival" [43]. Furthermore, our analyses of gene expression data from rodent models of TBI showed early elevation of BDNF, although temporal differences were noted across species, perhaps reflective of different models employed. Although Liddelow et al. [21] did not address the expression of *Bdnf*, when we examined their relevant genomic dataset of reactive astrogliosis (middle cerebral artery occlusion [27]), it was of appreciable interest to note that they found *Bdnf* expression was increased only at the early time point (24 h) examined whereas *Gfap* remained elevated over the whole time-course studied. Together these observations appear to be suggestive of the association of BDNF with a "good/beneficial" A2-like astrocyte early in injury to maintain brain homeostasis and signalling.

The Morphology of the A1 Phenotype of GFAP+ Astrocyte

Astrocytogenesis is the generation of astrocytes from neural stem cells and progenitor cells in the mammalian central

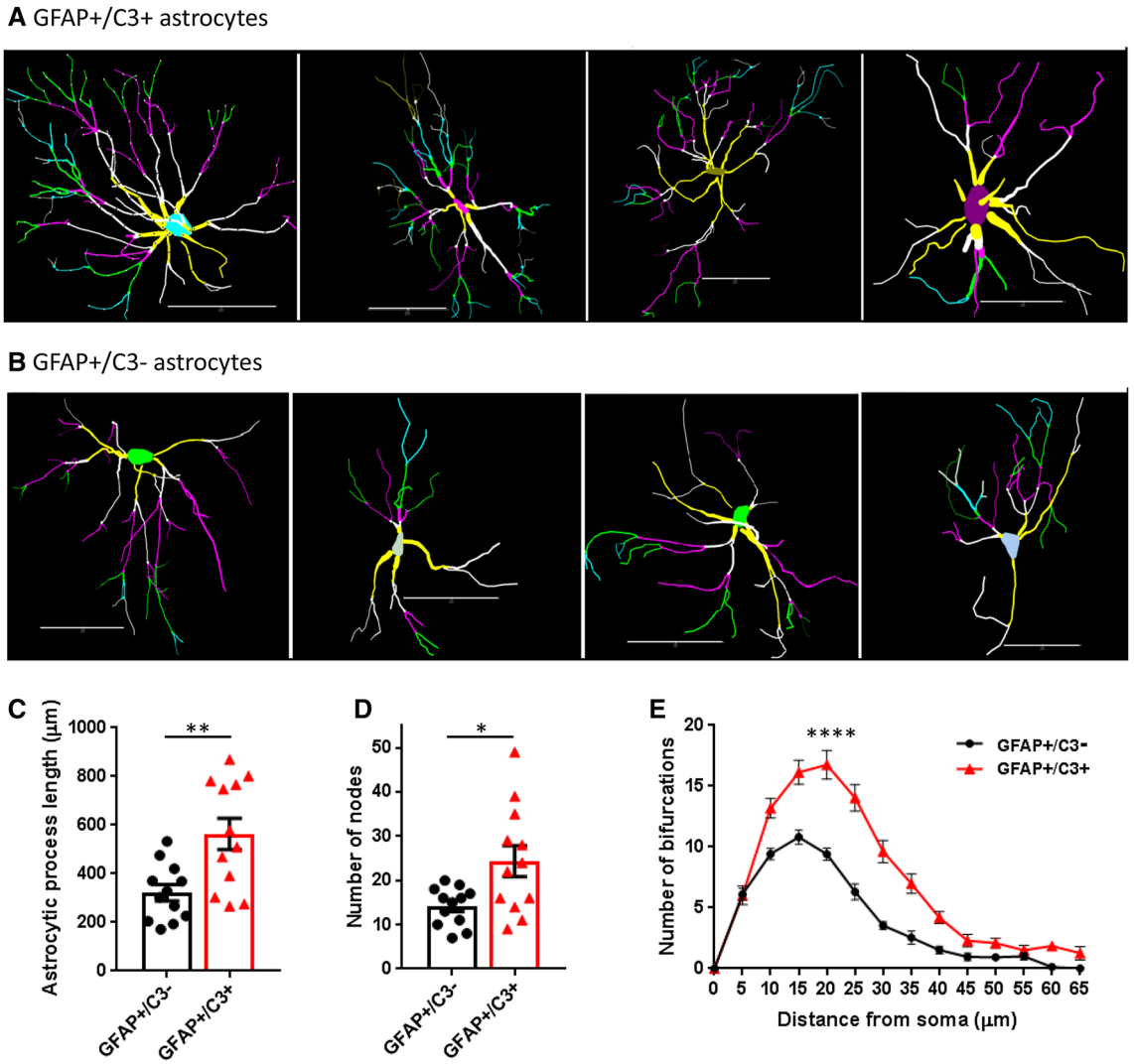

Fig. 4 Morphological comparison between GFAP+/C3+ to GFAP+/C3− labelled astrocytes. 3D reconstruction of processes extended by astrocytes was visualized and traced across the depth of histological sections with the Neurolucida software. Colour codes were used to identify primary and higher order branches. **a** GFAP+/C3− astrocytes and **b** GFAP+/C3+ astrocytes. Scale bar shown is 20 µm. **c** Quantification of the total length of astrocytic process tracings shown for GFAP+/C3− and GFAP+/C3+ (mean ± SEM, Mann–Whitney *t* test was performed). **d** Quantification of the total number of nodes of astrocytic process tracings shown for GFAP+/C3− and GFAP+/C3+ (mean ± SEM, Mann–Whitney *t* test was performed). **e** Sholl analysis of arbour tracings (mean ± SEM, Kruskal–Wallis test with Dunn's post hoc comparisons). Significant differences *($p < 0.05$) were observed for astrocytic process length; **($p < 0.01$) for number of nodes, and ****($p < 0.0001$) for the number of bifurcations for GFAP+/C3− and GFAP+/C3+ astrocytes

nervous system [44]. Following a brain injury, the proliferating population of neural stem cells and progenitor cells is exposed to numerous cytokines and growth factors. This process must be tightly regulated because an abnormal increase in the number of astrocytes after brain injury (astrogliosis, also known as astrocytosis or reactive astrocytosis) can cause scar formation and, in severe cases, inhibition of axon regeneration [45].

A1 astrocyte morphology is shown to vary drastically as indicated in different human neurodegeneration models [21]. In Huntington's and Alzheimer's disease models in humans, C3 accumulates in clusters and is expressed in the nucleus of astrocytes. In the present study, the expression of C3 in a rat TBI resembles Parkinson's disease and multiple sclerosis in humans, in which C3 organises along the processes and body of hypertrophic astrocytes (Fig. 3a). Due to the high background of the antibody used, whether there are smaller astrocytes with thinly defined processes also express C3 is not known. Comparable future studies that use super resolution or confocal microscopy to examine C3 expression using a primary antibody raised in a different host or targeting a different terminus of the protein are needed to

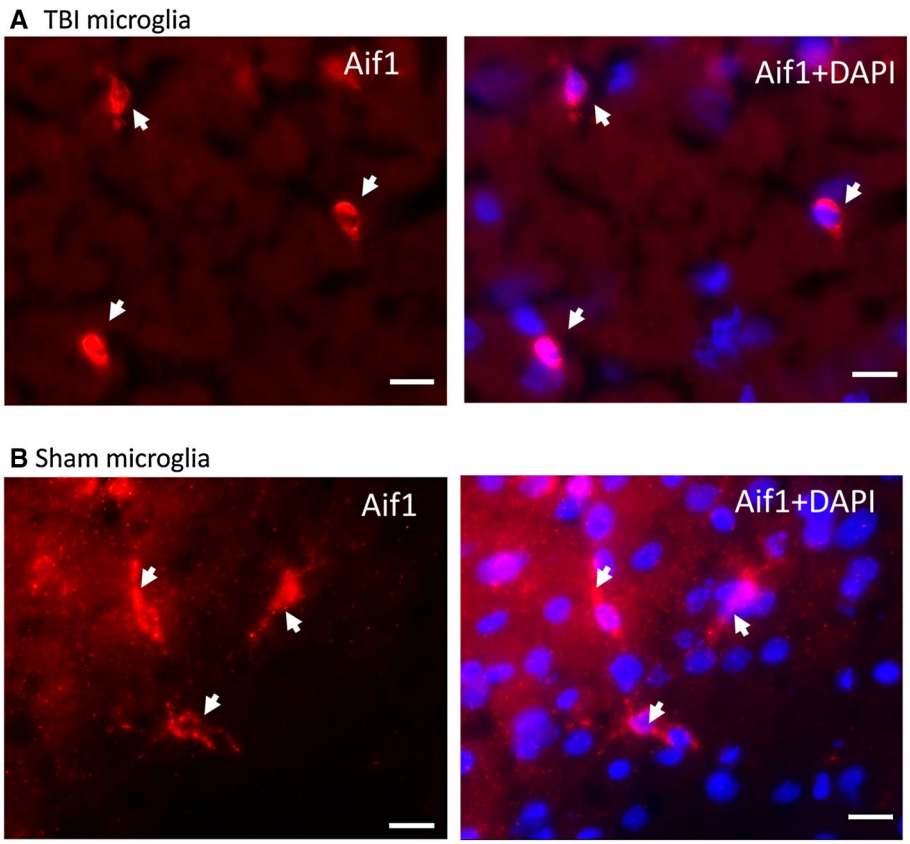

Fig. 5 Immunofluorescent labelling of Aif1/Iba1 in the somatosensory cortex of **a** TBI; **b** Sham rats. Immunolabelled for Aif1/Iba1 (red) and stained by DAPI (blue); merged images showing the Aif1/Iba1 are localised outside the nucleus. Arrow heads indicate microglia of interest. All scale bars shown are 20 µm. Alex Fluor 488 green signal was digitally converted to red signal. Images show representative example of results obtained on n = 5 mice

be conclusive about the morphology of the A1 astrocyte in brain injury models. Nevertheless, astrocytes expressing C3 when traced in real-time using the software Neurolucida showed a more elaborated and bigger arbour compared to the astrocytes that did not co-label with C3. However, the astrocyte marker GFAP only labels the main branches of astrocytes [11], hence differences between a resting astrocyte and an A1 astrocyte in terms of arbour complexity more distal to the soma of the astrocyte need to be interpreted with caution. This observed increase in arbour complexity may also be a consequence of an elevated GFAP expression rather than an actual increase in arbour size. Future studies including cell tracing using Golgi stained astrocytes would give a further insight of morphological changes associated with the A1 phenotype.

Microglia Phenotypes—Function and Dysfunction

Microglia are the brain's primary resident immune cells and whilst not a prime focus of the early phase of this work, we did find supportive evidence for microglial morphology changes in response to TBI, as previously reported [5] and our future endeavours will address any changes in cell populations and functions. Derived from primitive yolk sac macrophages, they play a key role in regulating brain development through a number of mechanisms, primarily involving the release of factors and phagocytosis (reviewed in [46]). Microglia have been implicated in myelination, neurogenesis, synaptic formation and maturation in the developing brain whilst they are also known to be involved in the phagocytosis of neural progenitors and synapses. In the adult brain, under normal homeostatic conditions, microglia are constantly surveying their environment. In fact, they are highly responsive to perturbations in their microenvironment with factors such as CSF-1 and TGF-β influencing their phenotype. The term "microglial polarisation" has been coined to define these neurotoxic 'M1' and neuroprotective 'M2' phenotypes [47]. However, this classification is now considered outdated and an oversimplification of the CNS in vivo [48]. The M1/M2 classification was largely derived from data obtained from highly simplified contexts using isolated cells of a single type and treating with purified stimuli such a lipopolysaccharide/interferon gamma or IL4/13. However, in vivo, damage-associated molecular patterns (DAMPs) released by damaged neurons and cytokines and other signalling mediators released from astrocytes are also potent stimuli of microglia. These complex interactions with other cell types within the brain are not accurately mimicked in these in vitro studies and are one of the concerns when directly translating these findings to more complex in vivo models including trauma, infection, inflammation, ischemia and neurodegeneration. This M1/M2 classification

of microglia also fails to consider other complexities including the transcriptomic and proteomic profiles, heterogeneity between brain regions, sex differences, and functional changes associated with aging [49]. A recent single-cell RNA analysis of CNS immune cells in neurodegenerative conditions identified a subset of disease-associated microglia (DAM) that showed a unique transcriptional and functional signature that was conserved in mice and humans [50]. It is also known that aged microglia display differential gene expression, termed a "microglial sensome" [51]. Aging also influences microglial function, with decreased phagocytic activity and a reduced threshold of microglial priming by immune stimuli [52]. Brain-region differences in microglial gene transcription have also been reported [53]. The influence of this microglial heterogeneity on the brain's immune response to injury or infection is still not fully understood.

Following a TBI, microglia activation is an early event with morphological and electrophysiological changes and increases in proliferation and migration, with this occurring in multiple phases (reviewed in [54]). In humans, chronically activated microglia have been linked to the tissue degeneration observed years after the initial injury [1, 55]. In rodent models of TBI, sustained microglial activation has also been associated with the neuronal loss. In focal brain injury models, microglia respond within minutes by projecting their processes to the site of damage [56, 57], while in concussion models, microgliosis (and astrocytosis) have been reported at early and late time points after injury [58, 59]. Microglial activation has also been reported in blast injury models [60]. Gene expression profiling of brain tissue in TBI has suggested a potential role for the damaging inflammatory response in contributing to the severity and extent of the injury, however the studies thus far have been limited to whole brain tissue [61]. Indeed, although considered to be neurotoxic following a TBI, microglia can also play a neuroprotective role, particularly in the acute phase of injury, through the phagocytic clean-up of dead cells and by assisting in the maintenance of the glial limitans and vasculature to ultimately promote remodelling and repair (reviewed in [4]). In addition, although evidence suggests some redundancy in the inflammatory gene expression between various models (for example, FPI and mild CCI, single versus repeated injury), there are differences in the duration and magnitude of the response and the location from the injury site (reviewed in [62]). In fact, these models have also demonstrated mixed expression of M1 and M2 phenotypic markers (reviewed in [63]), again raising questions regarding the simplification of this classification to denote microglial responses in TBI. RNAseq at the single cell level in models of TBI will allow microglial profiles to be established at different regions of the brain over different time periods. Similar to that reported with neurodegenerative diseases such as Alzheimer's disease [64], it is likely that microglia transform through toxic and protective states following a TBI, with these inflammatory phenotypes influenced by communication with their surrounding cells, such as astrocytes. A greater understanding of the temporal changes following TBI at both the gene and cellular level is therefore required to gain a greater understanding of the inflammatory response following TBI.

Microglial–Astrocytic Crosstalk

Following a TBI, the acute immune response involving microglia and astrocytes has been shown to be necessary for repair and remodelling and also in the maintenance of BBB integrity. In early studies TBI induced by laser ablation and mechanical injury, two-photon microscopy revealed microglial processes, but not their somata, are rapidly extended within a few minutes and after approximately 30 min reached the damaged site [65]. Further work using the laser ablation model demonstrated that astrocytes are polarized towards the injury with the establishment of a cytoplasmic Ca^{2+} gradient preceding the microglial response [66]. Herein the astrocytic involvement likely included release of ATP and GAP junction connexin hemichannels [65, 66]. This evidence supports early astrocytic–microglial crosstalk with microglial responses considered to involve an acute phase (0–30 min) and a slower phase of somata movement (1–3 days; [66]). More recent studies using two-photon laser scanning microscopy have demonstrated a key role for microglia in forming a honeycomb-like network within an hour post-injury in a closed-head model of mild TBI [57]. These structures lined the compromised glia limitans, and surrounded and protected the surviving astrocytes within the lesion to prevent further astrocytic death and dysfunction, neutrophil infiltration and neuronal loss. However, in TBI, the sustained activation of microglia and astrocytes can lead to enhanced tissue damage, and recent evidence suggests that this may be mediated by a crosstalk between the two cell types. Overall, whilst reactive astrocytes certainly undergo changes that vary with insult severity, they are documented to not only guide microglia to an injury but also to exert both pro- and anti-inflammatory effects on microglia [11, 66], evidence which when taken with the findings of Liddelow et al. [21] supports the multiple phases, likely bidirectionality and complexities of glial crosstalk.

Chronic microglial activation leads to the release of pro-inflammatory mediators such as IL1-β, TNFs and C1qa that are known to activate astrocytes to a highly neurotoxic A1 phenotype, cells which are characterised by increased C3 expression [21]. These cells induce neuronal cell death in contrast to the A2 reactive astrocytes which have been reported to promote neuronal survival and tissue repair in models of spinal cord injury [67, 68]. Functionally, A1 reactive astrocytes have lost their ability to promote neuronal

survival and outgrowth, promote synapse formation and to phagocytose synapses and debris. Therefore, not surprisingly, A1 reactive astrocytes have been detected in a variety of human neurodegenerative conditions, including multiple sclerosis, amyotrophic lateral sclerosis, Parkinson's and Alzheimer's diseases and specifically, were found in brain regions of disease. For example, in multiple sclerosis lesions, C3-positive astrocytes were in close proximity to CD68 positive microglia, whilst in the prefrontal cortex of Alzheimer's disease patients, 60% of GFAP-positive astrocytes were also C3-positive [21]. Recently, akin to the "microglial sensome" reported in aging mouse and humans, aged brains have also been shown to express differential astrocytic gene expression [69]. Clarke et al. [70] specifically linked the aging-induced upregulation of genes to a reactive A1 astrocyte phenotype that was absent in mice lacking lacking the microglial-secreted cytokines, IL-1α, TNF, and C1q. Recently, Yun et al. [71] reported that prevention of this microglial conversion of astrocytes to the A1 neurotoxic phenotype was neuroprotective in α-synuclein mouse models of Parkinson's disease. Despite the recent exciting work focusing on microglial activation being essential for the generation of toxic A1 astrocytes, one cannot help, when appraising the literature as a whole, from adopting the view that glial crosstalk is likely to be polymodal and dependent on the time-course and severity of the brain injury/disturbance. The role of A1 astrocytes and the influence of microglia on this neurotoxic phenotypic conversion have not been explored in TBI.

Astrocytic Phenotypes—Function and Dysfunction

Astrocytes, the most populous cells in the mammalian CNS, are highly polarized, multifunctional brain cells that perform critical roles in amino acid, metabolic, energetic, neurotrophin, anti-oxidant and ion function, being coupled to neuronal activity and cerebral blood flow, and modulation of excitatory synaptic transmission. From a signalling perspective, astrocytes were a generally forgotten partner until the emergence of the concept of the tripartite synapse [72]. For many years impaired astrocytic function has been known to worsen neuronal dysfunction after brain injury and gene knockout [45, 73]. Excitotoxicity, frequently evoked as an injury mechanism in many different types of brain pathologies, is intimately linked to the function of L-glutamate transporters, which are predominantly localized to the finer rather than major branches of the astrocytic arbour [74, 75]. This arbour is extensive, and features end-feet on vasculature, BBB and tight junctions with other astrocytes—this diversity contributes to the complexity of morphological changes and astrocytic plasticity noted especially in neuropathologies [19, 76]. Not only do astrocytes also modulate the activity of microglia [77–79], but they engage in the highly topical bidirectional microglial–astrocytic crosstalk (*vide infra*).

In central nervous system injury and disease, astrocytes exhibit diverse forms of response, which in severe or prolonged injury can be accompanied by their proliferation [45]. Thus astrocytogenesis is the generation of astrocytes from neural stem cells and progenitor cells in the mammalian central nervous system [44]. Following a brain injury, the proliferating population of neural stem cells and progenitor cells is exposed to numerous cytokines and growth factors. This process must be tightly regulated because an abnormal increase in the number of astrocytes after brain injury (astrogliosis/astrocytosis/reactive astrocytosis) can cause scar formation and, in severe cases, inhibition of axon regeneration [45]. In astrogliosis, astrocytes undergo rapid changes in morphology, gene expression and function. Studies over the last decade have revealed that in reality the continuum of responses, dependent upon the nature and severity of the insult/dysfunction, can be "good/beneficial" or "bad/disruptive" [73]. Seminal studies using gene knockout of GFAP and vimentin showed that changes to these cytoskeletal proteins resulted in astrocytes of a very different morphology, and reduced glial scarring with elevated inflammation pathological outcomes were also worsened, including for example in ischaemic injury where recovery was compromised [80]. Indeed, we previously found that it is possible by manipulation of the cytoskeleton of cultured astrocytes to generate a highly arbourised phenotype with less actin stress fibres and which we defined as a pro-survival phenotype because of its high expression of L-glutamate transporters, BDNF and anti-oxidant genes [43]. We took this concept of a "good/beneficial" astrocyte generated using the Rho kinase inhibitor Fasudil into a rat model of stroke injury and found less reactive astrocytes, reduced glial scarring and functional improvement [81]. The diversity of astrogliosis and its involvement in all forms of injury and disease had led to terminologies such as astrocytopathies, astrodegeneration and astroglial atrophy, which occur in various neurodegenerative conditions (see [13]).

In sum, our immunohistochemistry revealed for the first time that TBI triggered the expression of C3 i.e. the marker for toxic astrocytes. Our gene expression analyses confirmed that expression levels of GFAP and C3 were increased in the brain tissues containing the contusion area from fluid percussion injured rats or cortical controlled impacted mice. Nonetheless, it is possible that the temporal patterns of inflammatory gene expression and immune cell infiltration in other major TBI models (e.g. repetitive concussion, blast injury, rotational acceleration) may have unique inflammatory features. Furthermore, the gene expression of individual cells such as microglia or astrocytes has not been evaluated and should to be addressed in further studies of TBI using single cell RNAseq. Regardless, our finding of toxic

A1 astrocytes in TBI does emphasise that they represent an important target for new interventions in the management of the debilitating outcomes of TBI.

Acknowledgements PMB is pleased to contribute a paper to this Special Issue honouring Tony Turner who has been a colleague furthering the neurochemical cause via the Journal of Neurochemistry and internationally (ISN) and in Europe (ESN) for some 20 years. This work is partly funded by the J and M Nolan Family Trust. This work was supported by the Victorian Government through the Operational Infrastructure Scheme.

References

1. Johnson VE, Stewart W, Arena JD, Smith DH (2017) Traumatic brain injury as a trigger of neurodegeneration. Adv Neurobiol 15:383–400
2. Loane DJ, Stoica BA, Faden AI (2015) Neuroprotection for traumatic brain injury. Handb Clin Neurol 127:343–366
3. Faden AI, Wu J, Stoica BA, Loane DJ (2016) Progressive inflammation-mediated neurodegeneration after traumatic brain or spinal cord injury. Br J Pharmacol 173:681–691
4. Karve IP, Taylor JM, Crack PJ (2016) The contribution of astrocytes and microglia to traumatic brain injury. Br J Pharmacol 173:692–702
5. Fehily B, Fitzgerald M (2017) Repeated mild traumatic brain injury: potential mechanisms of damage. Cell Transplant 26:1131–1155
6. Sun M, McDonald SJ, Brady RD, O'Brien TJ, Shultz SR (2018) The influence of immunological stressors on traumatic brain injury. Brain Behav Immun 69:618–628
7. Ziebell JM, Morganti-Kossmann MC (2010) Involvement of pro- and anti-inflammatory cytokines and chemokines in the pathophysiology of traumatic brain injury. Neurotherapeutics 7:22–30
8. Kelso ML, Gendelman HE (2014) Bridge between neuroimmunity and traumatic brain injury. Curr Pharm Des 20:4284–4298
9. Corps KN, Roth TL, McGavern DB (2015) Inflammation and neuroprotection in traumatic brain injury. JAMA Neurol 72:355–362
10. Loane DJ, Byrnes KR (2010) Role of microglia in neurotrauma. Neurotherapeutics 7:66–77
11. Sofroniew MV, Vinters HV (2010) Astrocytes: biology and pathology. Acta Neuropathol 119:7–35
12. Barres BA (2008) The mystery and magic of glia: a perspective on their roles in health and disease. Neuron 60:430–440
13. Verkhratsky A, Zorec R, Rodriguez JJ, Parpura V (2017) Neuroglia: functional paralysis and reactivity in Alzheimer's disease and other neurodegenerative pathologies. Adv Neurobiol 15:427–449
14. Bao F, Shultz SR, Hepburn JD, Omana V, Weaver LC, Cain DP, Brown A (2012) A CD11d monoclonal antibody treatment reduces tissue injury and improves neurological outcome after fluid percussion brain injury in rats. J Neurotrauma 29:2375–2392
15. Webster KM, Wright DK, Sun M, Semple BD, Ozturk E, Stein DG, O'Brien TJ, Shultz SR (2015) Progesterone treatment reduces neuroinflammation, oxidative stress and brain damage and improves long-term outcomes in a rat model of repeated mild traumatic brain injury. J Neuroinflamm 12:238
16. Shultz SR, Sun M, Wright DK, Brady RD, Liu S, Beynon S, Schmidt SF, Kaye AH, Hamilton JA, O'Brien TJ, Grills BL, McDonald SJ (2015) Tibial fracture exacerbates traumatic brain injury outcomes and neuroinflammation in a novel mouse model of multitrauma. J Cereb Blood Flow Metab 35:1339–1347
17. Webster KM, Sun M, Crack P, O'Brien TJ, Shultz SR, Semple BD (2017) Inflammation in epileptogenesis after traumatic brain injury. J Neuroinflamm 14:10
18. Cafferty WB, Yang SH, Duffy PJ, Li S, Strittmatter SM (2007) Functional axonal regeneration through astrocytic scar genetically modified to digest chondroitin sulfate proteoglycans. J Neurosci 27:2176–2185
19. Ridet JL, Malhotra SK, Privat A, Gage FH (1997) Reactive astrocytes: cellular and molecular cues to biological function. Trends Neurosci 20:570–577
20. Anderson MA, Burda JE, Ren Y, Ao Y, O'Shea TM, Kawaguchi R, Coppola G, Khakh BS, Deming TJ, Sofroniew MV (2016) Astrocyte scar formation aids central nervous system axon regeneration. Nature 532:195–200
21. Liddelow SA, Guttenplan KA, Clarke LE, Bennett FC, Bohlen CJ, Schirmer L, Bennett ML, Münch AE, Chung WS, Peterson TC, Wilton DK, Frouin A, Napier BA, Panicker N, Kumar M, Buckwalter MS, Rowitch DH, Dawson VL, Dawson TM, Stevens B, Barres BA (2017) Neurotoxic reactive astrocytes are induced by activated microglia. Nature 541:481–487
22. Sewell DL, Nacewicz B, Liu F, Macvilay S, Erdei A, Lambris JD, Sandor M, Fabry Z (2004) Complement C3 and C5 play critical roles in traumatic brain cryoinjury: blocking effects on neutrophil extravasation by C5a receptor antagonist. J Neuroimmunol 155:55–63
23. Loane DJ, Kumar A (2016) Microglia in the TBI brain: the good, the bad, and the dysregulated. Exp Neurol 275:316–327
24. Kumar A, Alvarez-Croda DM, Stoica BA, Faden AI, Loane DJ (2016) Microglial/macrophage polarization dynamics following traumatic brain injury. J Neurotrauma 33:1732–1750
25. Kreutzberg GW (1996) Microglia: a sensor for pathological events in the CNS. Trends Neurosci 19:312–318
26. Hanisch UK, Kettenmann H (2007) Microglia: active sensor and versatile effector cells in the normal and pathologic brain. Nat Neurosci 10:1387–1394
27. Zamanian JL, Xu L, Foo LC, Nouri N, Zhou L, Giffard RG, Barres BA (2012) Genomic analysis of reactive astrogliosis. J Neurosci 32:6391–6410
28. Burda JE, Sofroniew MV (2017) Seducing astrocytes to the dark side. Cell Res 27:726–727
29. Natale JE, Ahmed F, Cernak I, Stoica B, Faden AI (2003) Gene expression profile changes are commonly modulated across models and species after traumatic brain injury. J Neurotrauma 20:907–927
30. Barrett T, Wilhite SE, Ledoux P, Evangelista C, Kim IF, Tomashevsky M, Marshall KA, Phillippy KH, Sherman PM, Holko M, Yefanov A, Lee H, Zhang N, Robertson CL, Serova N, Davis S, Soboleva A (2013) NCBI GEO: archive for functional genomics data sets—update. Nucleic Acids Res 41:D991–D995
31. Bolstad BM, Irizarry RA, Astrand M, Speed TP (2003) A comparison of normalization methods for high density oligonucleotide array data based on bias and variance. Bioinformatics 19:185–193
32. RStudio Team (2015) RStudio: integrated development for R. RStudio, Inc., Boston
33. Wickham H (2009) ggplot2: elegant graphics for data analysis. Springer, New York
34. Kent WJ (2002) BLAT—the BLAST-like alignment tool. Genome Res 12:656–664
35. Kent WJ, Sugnet CW, Furey TS, Roskin KM, Pringle TH, Zahler AM, Haussler D (2002) The human genome browser at UCSC. Genome Res 12:996–1006
36. Shultz SR, Cardamone L, Liu YR, Hogan RE, Maccotta L, Wright DK, Zheng P, Koe A, Gregoire MC, Williams JP, Hicks RJ, Jones NC, Myers DE, O'Brien TJ, Bouilleret V (2013) Can structural or functional changes following traumatic brain injury in the rat predict epileptic outcome? Epilepsia 54:1240–1250

37. Johnstone VP, Wright DK, Wong KK, O'Brien TJ, Rajan R, Shultz S (2015) Experimental traumatic brain injury results in long-term recovery of functional responsiveness in sensory cortex but persisting structural changes and sensorimotor, cognitive, and emotional deficits. J Neurotrauma 32:1333–1346
38. Wright DK, Liu S, van der Poel C, McDonald SJ, Brady RD, Taylor L, Yang L, Gardner AJ, Ordidge R, O'Brien TJ, Johnston LA, Shultz SR (2017) Traumatic brain injury results in cellular, structural and functional changes resembling motor neuron disease. Cereb Cortex 27:4503–4515
39. Paxinos G, Watson C (2007) The rat brain in stereotaxic coordinates. Academic Press, San Diego
40. Ziebell JM, Taylor SE, Cao T, Harrison JL, Lifshitz J (2012) Rod microglia: elongation, alignment, and coupling to form trains across the somatosensory cortex after experimental diffuse brain injury. J Neuroinflamm 9:247
41. Gundersen HJ, Jensen EB (1987) The efficiency of systematic sampling in stereology and its prediction. J Microsc 147:229–263
42. Schmitz C, Hof PR (2005) Design-based stereology in neuroscience. Neuroscience 130:813–831
43. Lau CL, Perreau VM, Chen MJ, Cate HS, Merlo D, Cheung NS, O'Shea RD, Beart PM (2012) Transcriptomic profiling of astrocytes treated with the Rho kinase inhibitor fasudil reveals cytoskeletal and pro-survival responses. J Cell Physiol 227:1199–1211
44. Namihira M, Nakashima K (2013) Mechanisms of astrocytogenesis in the mammalian brain. Curr Opin Neurobiol 23:921–927
45. Sofroniew MV (2009) Molecular dissection of reactive astrogliosis and glial scar formation. Trends Neurosci 32:638–647
46. Lenz KM, Nelson LH (2018) Microglia and beyond: innate immune cells as regulators of brain development and behavioral function. Front Immunol 9:698
47. Colton CA (2009) Heterogeneity of microglial activation in the innate immune response in the brain. J Neuroimmune Pharmacol 4:399–418
48. Sarlus H, Heneka MT (2017) Microglia in Alzheimer's disease. J Clin Investig 127:3240–3249
49. Ransohoff RM (2016) A polarizing question: do M1 and M2 microglia exist? Nat Neurosci 19:987–991
50. Keren-Shaul H, Spinrad A, Weiner A, Matcovitch-Natan O, Dvir-Szternfeld R, Ulland TK, David E, Baruch K, Lara-Astaiso D, Toth B, Itzkovitz S, Colonna M, Schwartz M, Amit I (2017) A unique microglia type associated with restricting development of Alzheimer's disease. Cell 169:1276–1290
51. Hickman SE, Kingery ND, Ohsumi TK, Borowsky ML, Wang LC, Means TK, El Khoury J (2013) The microglial sensome revealed by direct RNA sequencing. Nat Neurosci 16:1896–1905
52. Deczkowska A, Keren-Shaul H, Weiner A, Colonna M, Schwartz M, Amit I (2018) Disease-associated microglia: a universal immune sensor of neurodegeneration. Cell 173:1073–1081
53. Grabert K, Michoel T, Karavolos MH, Clohisey S, Baillie JK, Stevens MP, Freeman TC, Summers KM, McColl BW (2016) Microglial brain region-dependent diversity and selective regional sensitivities to aging. Nat Neurosci 19:504–516
54. Jassam YN, Izzy S, Whalen M, McGavern DB, El Khoury J (2017) Neuroimmunology of traumatic brain injury: time for a paradigm shift. Neuron 95:1246–1265
55. Ramlackhansingh AF, Brooks DJ, Greenwood RJ, Bose SK, Turkheimer FE, Kinnunen KM, Gentleman S, Heckemann RA, Gunanayagam K, Gelosa G, Sharp DJ (2011) Inflammation after trauma: microglial activation and traumatic brain injury. Ann Neurol 70:374–383
56. Fourgeaud L, Través PG, Tufail Y, Leal-Bailey H, Lew ED, Burrola PG, Callaway P, Zagórska A, Rothlin CV, Nimmerjahn A, Lemke G (2016) TAM receptors regulate multiple features of microglial physiology. Nature 532:240–244
57. Roth TL, Nayak D, Atanasijevic T, Koretsky AP, Latour LL, McGavern DB (2014) Transcranial amelioration of inflammation and cell death after brain injury. Nature 505:223–228
58. Shitaka Y, Tran HT, Bennett RE, Sanchez L, Levy MA, Dikranian K, Brody DL (2011) Repetitive closed-skull traumatic brain injury in mice causes persistent multifocal axonal injury and microglial reactivity. J Neuropathol Exp Neurol 70:551–567
59. Mannix R, Meehan WP, Mandeville J, Grant PE, Gray T, Berglass J, Zhang J, Bryant J, Rezaie S, Chung JY, Peters NV, Lee C, Tien LW, Kaplan DL, Feany M, Whalen M (2013) Clinical correlates in an experimental model of repetitive mild brain injury. Ann Neurol 74:65–75
60. Huber BR, Meabon JS, Hoffer ZS, Zhang J, Hoekstra JG, Pagulayan KF, McMillan PJ, Mayer CL, Banks WA, Kraemer BC, Raskind MA, McGavern DB, Peskind ER, Cook DG (2016) Blast exposure causes dynamic microglial/macrophage responses and microdomains of brain microvessel dysfunction. Neuroscience 319:206–220
61. Meng Q, Zhuang Y, Ying Z, Agrawal R, Yang X, Gomez-Pinilla F (2017) Traumatic brain injury induces genome-wide transcriptomic, methylomic, and network perturbations in brain and blood predicting neurological disorders. EBioMedicine 16:184–194
62. Chiu CC, Liao YE, Yang LY, Wang JY, Tweedie D, Karnati HK, Greig NH, Wang JY (2016) Neuroinflammation in animal models of traumatic brain injury. J Neurosci Methods 272:49
63. Donat CK, Scott G, Gentleman SM, Sastre M (2017) Microglial activation in traumatic brain injury. Front Aging Neurosci 9:208
64. Bouvier DS, Murai KK (2015) Synergistic actions of microglia and astrocytes in the progression of Alzheimer's disease. J Alzheimers Dis 45:1001–1014
65. Davalos D, Grutzendler J, Yang G, Kim JV, Zuo Y, Jung S, Littman DR, Dustin ML, Gan WB (2005) ATP mediates rapid microglial response to local brain injury in vivo. Nat Neurosci 8:752–758
66. Kim JV, Dustin ML (2006) Innate response to focal necrotic injury inside the blood-brain barrier. J Immunol 177:5269–5277
67. Faulkner JR, Herrmann JE, Woo MJ, Tansey KE, Doan NB, Sofroniew MV (2004) Reactive astrocytes protect tissue and preserve function after spinal cord injury. J Neurosci 24:2143–2155
68. Herrmann JE, Imura T, Song B, Qi J, Ao Y, Nguyen TK, Korsak RA, Takeda K, Akira S, Sofroniew MV (2008) STAT3 is a critical regulator of astrogliosis and scar formation after spinal cord injury. J Neurosci 28:7231–7243
69. Boisvert MM, Erikson GA, Shokhirev MN, Allen NJ (2018) The aging astrocyte transcriptome from multiple regions of the mouse brain. Cell Rep 22:269–285
70. Clarke LE, Liddelow SA, Chakraborty C, Münch AE, Heiman M, Barres BA (2018) Normal aging induces A1-like astrocyte reactivity. Proc Natl Acad Sci USA 115:E1896–E1905
71. Yun SP, Kam TI, Panicker N, Kim S, Oh Y, Park JS, Kwon SH, Park YJ, Karuppagounder SS, Park H, Kim S, Oh N, Kim NA, Lee S, Brahmachari S, Mao X, Lee JH, Kumar M, An D, Kang SU, Lee Y, Lee KC, Na DH, Kim D, Lee SH, Roschke VV, Liddelow SA, Mari Z, Barres BA, Dawson VL, Lee S, Dawson TM, Ko HS (2018) Block of A1 astrocyte conversion by microglia is neuroprotective in models of Parkinson's disease. Nat Med 24:931–938
72. Araque A, Parpura V, Sanzgiri RP, Haydon PG (1999) Tripartite synapses: glia, the unacknowledged partner. Trends Neurosci 22:208–215
73. Sofroniew MV (2015) Astrocyte barriers to neurotoxic inflammation. Nat Rev Neurosci 16:249–263
74. Beart PM, O'Shea RD (2007) Transporters for L-glutamate: an update on their molecular pharmacology and pathological involvement. Br J Pharmacol 150:5–17

75. Martinez-Lozada Z, Guillem AM, Robinson MB (2016) Transcriptional regulation of glutamate transporters: from extracellular signals to transcription factors. Adv Pharmacol 76:103–145
76. Panickar KS, Norenberg MD (2005) Astrocytes in cerebral ischemic injury: morphological and general considerations. Glia 50:287–298
77. Schipke CG, Boucsein C, Ohlemeyer C, Kirchhoff F, Kettenmann H (2002) Astrocyte Ca^{2+} waves trigger responses in microglial cells in brain slices. FASEB J 16:255–257
78. Verderio C, Matteoli M (2001) ATP mediates calcium signaling between astrocytes and microglial cells: modulation by IFN-gamma. J Immunol 166:6383–6391
79. Norden DM, Fenn AM, Dugan A, Godbout JP (2014) TGFß produced by IL-10 redirected astrocytes attenuates microglial activation. Glia 62:881–895
80. Li L, Lundkvist A, Andersson D, Wilhelmsson U, Nagai N, Pardo AC, Nodin C, Ståhlberg A, Aprico K, Larsson K, Yabe T, Moons L, Fotheringham A, Davies I, Carmeliet P, Schwartz JP, Pekna M, Kubista M, Blomstrand F, Maragakis N, Nilsson M, Pekny M (2008) Protective role of reactive astrocytes in brain ischemia. J Cereb Blood Flow Metab 28:468–481
81. Abeysinghe HC, Phillips EL, Chin-Cheng H, Beart PM, Roulston CL (2016) Modulating astrocyte transition after stroke to promote brain rescue and functional recovery: emerging targets include rho kinase. Int J Mol Sci 17:288–305